Traffic Flow Reconstruction between PDEs and Machine Learning

Nail Baloul, Amaury Hayat, Thibault Liard, Pierre Lissy[1]

English Math Seminar, Algiers

October, 6th 2025

[1] N. Baloul, A. Hayat, and P. Lissy are with CERMICS, École nationale des ponts et chaussées, France
Thibault Liard is with XLIM, Université de Limoges, France

In Memory of Professor Ammar Khemmoudj

(1956–2024)

With gratitude for his inspiration, guidance,
and dedication to education.

"His impact on our lives and work will always be remembered."

Outline

Table of Contents

Motivation

Traffic jam in Beijing

- Traffic congestion is a main contributor of air pollution and excessive travel time
  $\Rightarrow$ impacts urban mobility and environmental quality

Motivation

Traffic jam in Beijing

- Traffic congestion is a main contributor of air pollution and excessive travel time
  $\Rightarrow$ impacts urban mobility and environmental quality
- Traffic management relies on **control** schemes to address perturbed traffic conditions
- Most existing control techniques require complete and accurate knowledge of state
- In practice, full information is rarely available due to limited and noisy measurements

Motivation

Traffic jam in Beijing

- Traffic congestion is a main contributor of air pollution and excessive travel time
  $\Rightarrow$ impacts urban mobility and environmental quality
- Traffic management relies on **control** schemes to address perturbed traffic conditions
- Most existing control techniques require complete and accurate knowledge of state
- In practice, full information is rarely available due to limited and noisy measurements
- $\boxed{\textbf{Goal} \Rightarrow \text{develop reliable methods for } \textbf{estimating traffic from partial data}}$

Traffic Flow Modeling Scales

Benchmark scales of traffic models

- microscopic $\Rightarrow$ individual vehicle dynamics, full information given

Microscopic model

- Simulation of agent-based dynamics
- Tracking position $x_i(t)$, velocity $v_i(t)$ of vehicle i at time t
- Each driver responds to surrounding traffic by adjusting his speed

$$\dot{v}_i(t) = F(v_i(t), x_i(t)) \tag{1}$$

[2] Di Francesco, Fagioli, Rosini, and Russo 2016.

Benchmark scales of traffic models

- macroscopic $\Rightarrow$ continuum representation using aggregated variables

Macroscopic model

- Traffic modelled as a continuous flow
- Density $\rho(t,x)$, speed $v(\rho)$, flux $f(\rho)$
- Total number of cars is conserved

$$\begin{aligned} 0 =& \frac{d}{dt}\int_a^b \rho(t,x)dx \\ =& f(\rho(t,a)) - f(\rho(t,b)) \\ =& -\int_a^b \frac{\partial}{\partial x} f(\rho(t,x))dx \end{aligned} \tag{2}$$

[2] Di Francesco, Fagioli, Rosini, and Russo 2016.

Traffic Flow Modeling Scales

Benchmark scales of traffic models

- microscopic $\Rightarrow$ individual vehicle dynamics, full information given
- macroscopic $\Rightarrow$ continuum representation using aggregated variables

Microscopic model

- Simulation of agent-based dynamics
- Tracking position $x_i(t)$, velocity $v_i(t)$ of vehicle i at time t
- Each driver responds to surrounding traffic by adjusting his speed

$$\dot{v}_i(t) = F(v_i(t), x_i(t)) \tag{1}$$

Macroscopic model

- Traffic modelled as a continuous flow
- Density $\rho(t,x)$, speed $v(\rho)$, flux $f(\rho)$
- Total number of cars is conserved

$$\begin{aligned} 0 &= \frac{d}{dt}\int_a^b \rho(t,x)dx \\ &= f(\rho(t,a)) - f(\rho(t,b)) \\ &= -\int_a^b \frac{\partial}{\partial x} f(\rho(t,x))dx \end{aligned} \tag{2}$$

- **Connection** $\Rightarrow$ macroscopic variables emerge from microscopic interactions[2]

[2] Di Francesco, Fagioli, Rosini, and Russo 2016.

Microscopic Model

- 2 quantities -which only depends on time- used to describe traffic systems
  $\Rightarrow$ state x_i (position of vehicle i at time t)
  $\Rightarrow$ velocity v_i (speed of vehicle i at time t)

Microscopic Model

- 2 quantities -which only depends on time- used to describe traffic systems
  $\Rightarrow$ state x_i (position of vehicle i at time t)
  $\Rightarrow$ velocity v_i (speed of vehicle i at time t)
- Dynamics depend on **headway** $\Rightarrow$ captures reaction effects explicitly

$$\dot{x}_i(t) = v(z_i(t)) \tag{3}$$

where $z_i(t)$ accounts for surrounding of vehicle i

Macroscopic Model

- 3 quantities -which all depend on space and time- used to describe traffic systems
  $\Rightarrow$ relative density ρ (number of vehicles per unit of length)
  $\Rightarrow$ average velocity v (mean speed of vehicles on a road segment)
  $\Rightarrow$ flow rate f (number of vehicles passing across a portion of the road during a period of time)

- 3 quantities -which all depend on space and time- used to describe traffic systems
  $\Rightarrow$ relative density ρ (number of vehicles per unit of length)
  $\Rightarrow$ average velocity v (mean speed of vehicles on a road segment)
  $\Rightarrow$ flow rate f (number of vehicles passing across a portion of the road during a period of time)
- **Fundamental diagram** of traffic flow $\Rightarrow f(\rho) = \rho V(\rho)$

- 3 quantities -which all depend on space and time- used to describe traffic systems
  $\Rightarrow$ relative density ρ (number of vehicles per unit of length)
  $\Rightarrow$ average velocity v (mean speed of vehicles on a road segment)
  $\Rightarrow$ flow rate f (number of vehicles passing across a portion of the road during a period of time)
- **Fundamental diagram** of traffic flow $\Rightarrow f(\rho) = \rho V(\rho)$
- **Hydrodynamic equation** and **conservation law** lead to LWR model

$$\rho_t + (\rho V(\rho))_x = 0 \tag{4}$$

where $V(\rho)$ is the **equilibrium** velocity
$\Rightarrow$ assumes that in any given situation, vehicles immediately adjust their velocity to match the equilibrium velocity dictated by density $v(t,x) = V(\rho)$
$\Rightarrow$ neglects acceleration effects and assumes traffic flow behaves as a compressible fluid

Table of Contents

Model-Based Approaches

- Follow-the-Leader (FtL), **microscopic** first order model
  $\Rightarrow$ dynamics of each vehicle depend on vehicle immediately in front

$$\begin{cases} \dot{x}_N^N(t) = v_{\max}, & t > 0, \\ \dot{x}_i^N(t) = v\left(\frac{L}{N(x_{i+1}^N(t) - x_i^N(t))}\right), & t > 0, \quad i = 0, \cdots, N-1 \\ x_i^N(0) = \bar{x}_i^N, & i = 0, \cdots, N \end{cases} \tag{5}$$

$\Rightarrow$ accurate traffic representation, encodes individual movements

$\Rightarrow$ computationally demanding, requires more data

Model-Based Approaches

- Follow-the-Leader (FtL), **microscopic** first order model
  $\Rightarrow$ dynamics of each vehicle depend on vehicle immediately in front

$$
\begin{cases}
\dot{x}_N^N(t) = v_{\max}, & t > 0, \\
\dot{x}_i^N(t) = v\left(\frac{L}{N(x_{i+1}^N(t) - x_i^N(t))}\right), & t > 0, \quad i = 0, \cdots, N-1 \\
x_i^N(0) = \bar{x}_i^N, & i = 0, \cdots, N
\end{cases}
\tag{5}
$$

  $\Rightarrow$ accurate traffic representation, encodes individual movements
  $\Rightarrow$ computationally demanding, requires more data

- Lighthill-William-Richards (LWR), **macroscopic** traffic flow model
  $\Rightarrow$ vehicles treated as a continuous medium similar to particles in fluid
  $\Rightarrow$ one-dimensional (hyperbolic) conservation law

$$
\begin{cases}
\frac{\partial}{\partial t}\rho(t,x) + \frac{\partial}{\partial x} f(\rho(t,x)) = 0, & x \in \mathbb{R}, \quad t > 0, \\
\rho(0,x) = \bar{\rho}(x), & x \in \mathbb{R}
\end{cases}
\tag{6}
$$

  $\Rightarrow$ faster implementation, less data-intensive
  $\Rightarrow$ overlooks traffic heterogeneity, oversimplifies traffic phenomena

- **Convergence analysis of FtL approximation scheme towards LWR model**[3]

[3] Holden and Risebro 2017.
[4] Di Francesco and Rosini 2015.

- **Convergence analysis of FtL approximation scheme towards LWR model**[3]
- Link between FtL and LWR based on atomization of initial density $\bar{\rho}$

$$\bar{x}_{i+1}^N := \sup\left\{x \in \mathbb{R} : \int_{\bar{x}_i^N}^{x} \bar{\rho}(y)dy = \frac{L}{N}\right\}, \quad i = 0, \cdots, N-1 \tag{7}$$

[3] Holden and Risebro 2017.

[4] Di Francesco and Rosini 2015.

Model-Based Approaches

- **Convergence analysis of FtL approximation scheme towards LWR model**[3]
- Link between FtL and LWR based on atomization of initial density $\bar{\rho}$

$$\bar{x}_{i+1}^N := \sup \left\{ x \in \mathbb{R} : \int_{\bar{x}_i^N}^{x} \bar{\rho}(y)dy = \frac{L}{N} \right\}, \quad i = 0, \cdots, N-1 \tag{7}$$

- Solution of PDE (5) can be recovered as many particle limit[4] of ODE system (6)

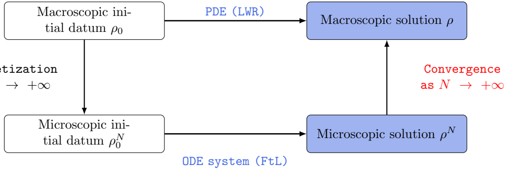

Coupled Resolution of a Microscopic ODE System and a Macroscopic PDE

[3] Holden and Risebro 2017.
[4] Di Francesco and Rosini 2015.

- Hybrid micro-macro models explored in traffic density reconstruction[5]

$$\begin{cases} \dot{x}_N^N(t) = v_{\max}, & t > 0, \\ \dot{x}_i^N(t) = v\left(\rho(t, x_i^N(t))\right), & t > 0,, \quad i = 0, \cdots, N-1 \\ \frac{\partial}{\partial t}\rho(t,x) + \frac{\partial}{\partial x} f(\rho(t,x)) = \gamma^2 \frac{\partial^2}{\partial x^2}\rho(t,x), & x \in \mathbb{R}, \quad t > 0, \quad \gamma^6 > 0 \end{cases} \tag{8}$$

[5] Barreau, Aguiar, Liu, and Johansson 2021.

[6] $\gamma > 0$ is a diffusion correction parameter. Hopf proved that as γ tends to zero, the solution of LWR with diffusion term converges in the sense of distributions to the solution of classical LWR.

[7] Liu, Barreau, Cicic, and Johansson 2020.

Data-Driven Approaches

- Hybrid micro-macro models explored in traffic density reconstruction[5]

$$\begin{cases} \dot{x}_N^N(t) = v_{\max}, & t > 0, \\ \dot{x}_i^N(t) = v\left(\rho(t, x_i^N(t))\right), & t > 0,, \quad i = 0, \cdots, N-1 \\ \frac{\partial}{\partial t}\rho(t,x) + \frac{\partial}{\partial x} f(\rho(t,x)) = \gamma^2 \frac{\partial^2}{\partial x^2}\rho(t,x), & x \in \mathbb{R}, \quad t > 0, \quad \gamma^6 > 0 \end{cases} \tag{8}$$

- **Partial state reconstruction**[7] using measurements from probe vehicles (PVs)
  $\Rightarrow$ low penetration rate $N_{\text{probes}} \ll N_{\text{total}}$
  $\Rightarrow$ recover density ρ from **limited** trajectories

[5] Barreau, Aguiar, Liu, and Johansson 2021.
[6] $\gamma > 0$ is a diffusion correction parameter. Hopf proved that as γ tends to zero, the solution of LWR with diffusion term converges in the sense of distributions to the solution of classical LWR.
[7] Liu, Barreau, Cicic, and Johansson 2020.

- Hybrid micro-macro models explored in traffic density reconstruction[5]

$$\begin{cases} \dot{x}_N^N(t) = v_{\max}, & t > 0, \\ \dot{x}_i^N(t) = v\left(\rho(t, x_i^N(t))\right), & t > 0,, \quad i = 0, \cdots, N-1 \\ \frac{\partial}{\partial t}\rho(t,x) + \frac{\partial}{\partial x} f(\rho(t,x)) = \gamma^2 \frac{\partial^2}{\partial x^2}\rho(t,x), & x \in \mathbb{R}, \quad t > 0, \quad \gamma^6 > 0 \end{cases} \tag{8}$$

- **Partial state reconstruction**[7] using measurements from probe vehicles (PVs)
  $\Rightarrow$ low penetration rate $N_{\text{probes}} \ll N_{\text{total}}$
  $\Rightarrow$ recover density ρ from **limited** trajectories
- Requires access to real-time positions, densities and instantaneous speeds of PVs

[5] Barreau, Aguiar, Liu, and Johansson 2021.
[6] $\gamma > 0$ is a diffusion correction parameter. Hopf proved that as γ tends to zero, the solution of LWR with diffusion term converges in the sense of distributions to the solution of classical LWR.
[7] Liu, Barreau, Cicic, and Johansson 2020.

- Hybrid micro-macro models explored in traffic density reconstruction[5]

$$\begin{cases} \dot{x}_N^N(t) = v_{\max}, & t > 0, \\ \dot{x}_i^N(t) = v\left(\rho(t, x_i^N(t))\right), & t > 0,, \quad i = 0, \cdots, N-1 \\ \frac{\partial}{\partial t}\rho(t,x) + \frac{\partial}{\partial x} f(\rho(t,x)) = \gamma^2 \frac{\partial^2}{\partial x^2}\rho(t,x), & x \in \mathbb{R}, \quad t > 0, \quad \gamma^6 > 0 \end{cases} \tag{8}$$

- **Partial state reconstruction**[7] using measurements from probe vehicles (PVs)
  $\Rightarrow$ low penetration rate $N_{\text{probes}} \ll N_{\text{total}}$
  $\Rightarrow$ recover density ρ from **limited** trajectories
- Requires access to real-time positions, densities and instantaneous speeds of PVs
- Prior approaches rely on knowledge of initial density $\bar{\rho}$
  $\Rightarrow$ **No access** to this critical information, need to leverage available data

[5] Barreau, Aguiar, Liu, and Johansson 2021.
[6] $\gamma > 0$ is a diffusion correction parameter. Hopf proved that as γ tends to zero, the solution of LWR with diffusion term converges in the sense of distributions to the solution of classical LWR.
[7] Liu, Barreau, Cicic, and Johansson 2020.

Table of Contents

Parametrized Microscopic Model

- **Limited data scenario** $\Rightarrow$ only **initial and final** $\left\{\left(\bar{x}^N, \bar{y}^N\right)\right\}_{i=0}^{n}$ positions of PVs

Parametrized Microscopic Model

- **Limited data scenario** $\Rightarrow$ only **initial and final** $\left\{\left(\bar{x}^N, \bar{y}^N\right)\right\}_{i=0}^{n}$ positions of PVs
- **Enhanced** version of FtL scheme (5) adding a parameter
  $\Rightarrow$ α^N accounts for unobserved vehicles between consecutive PVs
  $\Rightarrow$ adjusts dynamics and allows varying levels of response
  $\Rightarrow$ bridges discrete (vehicle-level) dynamics to continuous (density-level) dynamics

- **Limited data scenario** $\Rightarrow$ only **initial and final** $\left\{\left(\bar{x}^N, \bar{y}^N\right)\right\}_{i=0}^{n}$ positions of PVs
- **Enhanced** version of FtL scheme (5) adding a parameter
  - $\Rightarrow$ α^N accounts for unobserved vehicles between consecutive PVs
  - $\Rightarrow$ adjusts dynamics and allows varying levels of response
  - $\Rightarrow$ bridges discrete (vehicle-level) dynamics to continuous (density-level) dynamics
- Parametrized ODE system with finite time horizon

$$\begin{cases} \dot{x}_n^N(t) = v_{\max}, & t \in (0, T] \\ \dot{x}_i^N(t) = v\left(\rho_i^N(t)\right), & t \in (0, T] \quad i = 0, \cdots, n-1 \\ x_i^N(0) = \bar{x}_i^N, & i = 0, \cdots, n \end{cases} \tag{9}$$

$\Rightarrow$ local discrete densities

$$\rho_i^N(t) := \frac{\alpha_i^N L}{N\left(x_{i+1}^N(t) - x_i^N(t)\right)}, \quad t \in (0, T], \quad i = 0, \cdots, n-1 \tag{10}$$

Parametrized Microscopic Model

- **Limited data scenario** $\Rightarrow$ only **initial and final** $\left\{\left(\bar{x}^N, \bar{y}^N\right)\right\}_{i=0}^{n}$ positions of PVs
- **Enhanced** version of FtL scheme (5) adding a parameter
  $\Rightarrow$ α^N accounts for unobserved vehicles between consecutive PVs
  $\Rightarrow$ adjusts dynamics and allows varying levels of response
  $\Rightarrow$ bridges discrete (vehicle-level) dynamics to continuous (density-level) dynamics
- Parametrized ODE system with finite time horizon

$$\begin{cases} \dot{x}_n^N(t) = v_{\max}, & t \in (0, T] \\ \dot{x}_i^N(t) = v\left(\rho_i^N(t)\right), & t \in (0, T] \quad i = 0, \cdots, n-1 \\ x_i^N(0) = \bar{x}_i^N, & i = 0, \cdots, n \end{cases} \tag{9}$$

$\Rightarrow$ local discrete densities

$$\rho_i^N(t) := \frac{\alpha_i^N L}{N\left(x_{i+1}^N(t) - x_i^N(t)\right)}, \quad t \in (0, T], \quad i = 0, \cdots, n-1 \tag{10}$$

- Piecewise constant Eulerian discrete density

$$\rho^N(t,x) := \sum_{i=0}^{N-1} \rho_i^N(t) \chi_{[x_i^N(t), x_{i+1}^N(t))}(x), \quad x \in \mathbb{R}, \quad t \in [0, T] \tag{11}$$

Well Posedness

- Assumptions on velocity

$$v \in C^1([0, +\infty)) \tag{12a}$$

$$v \text{ is decreasing on } [0, +\infty) \tag{12b}$$

$$v(0) = v_{\max} < \infty \tag{12c}$$

Well Posedness

- Assumptions on velocity

$$v \in C^1([0, +\infty)) \tag{12a}$$

$$v \text{ is decreasing on } [0, +\infty) \tag{12b}$$

$$v(0) = v_{\max} < \infty \tag{12c}$$

- Local existence and uniqueness of solution to (9) (for fixed α) via Picard-Lindelöf

Well Posedness

- Assumptions on velocity

$$v \in C^1([0,+\infty)) \tag{12a}$$
$$v \text{ is decreasing on } [0,+\infty) \tag{12b}$$
$$v(0) = v_{\max} < \infty \tag{12c}$$

- Local existence and uniqueness of solution to (9) (for fixed α) via Picard-Lindelöf
- Condition on initial car positions $\bar{x}_0^N < \bar{x}_1^N < \cdots < \bar{x}_{n-1}^N < \bar{x}_n^N$
  $\Rightarrow$ global existence

Lemma (Discrete maximum principle)

For solution $x(t)$ of (9) with v satisfying (12a)-(12c), for all $i = 0, \cdots, n-1$,

$$\frac{\alpha_i^N L}{NM} \le x_{i+1}^N(t) - x_i^N(t) \le \bar{x}_n^N - \bar{x}_0^N + (v_{\max} - v(M))\, t, \quad \forall t \in [0, T], \tag{13}$$

where $M := \max_i \left(\frac{\alpha_i^N L}{N(\bar{x}_{i+1}^N - \bar{x}_i^N)} \right)$

Sketch of proof

- Lower bound is satisfied at $t = 0$, aim at extending property for all times up to T

Sketch of proof

- Lower bound is satisfied at $t = 0$, aim at extending property for all times up to T
- Equivalent to show

$$\inf_{0<t\leq T} [x_{i+1}(t) - x_i(t)] \geq \frac{\alpha_i^N L}{NM}, \quad i = 0, \dots, n-1. \tag{14}$$

$\Rightarrow$ **recursive argument** (backward from $n-1$ to 0)

Sketch of proof

- Lower bound is satisfied at $t = 0$, aim at extending property for all times up to T
- Equivalent to show

$$\inf_{0<t\leq T} [x_{i+1}(t) - x_i(t)] \geq \frac{\alpha_i^N L}{NM}, \quad i = 0, \dots, n-1. \tag{14}$$

$\Rightarrow$ **recursive argument** (backward from $n-1$ to 0)

- Property is true for $i = n-1$

$$\begin{aligned} x_n(t) - x_{n-1}(t) =& \bar{x}_n - \bar{x}_{n-1} + \int_0^t \left(v_{\max} - v\left(\frac{\alpha_n^N L}{N(x_n(s) - x_{n-1}(s))} \right) \right) ds \\ \geq& \bar{x}_n - \bar{x}_{n-1} \geq \frac{\alpha_{n-1}^N L}{NM}. \end{aligned}$$

- Lower bound is satisfied at $t = 0$, aim at extending property for all times up to T
- Equivalent to show

$$\inf_{0<t\leq T} [x_{i+1}(t) - x_i(t)] \geq \frac{\alpha_i^N L}{NM}, \quad i = 0, \dots, n-1. \tag{14}$$

$\Rightarrow$ **recursive argument** (backward from $n-1$ to 0)

- Property is true for $i = n-1$

$$\begin{aligned} x_n(t) - x_{n-1}(t) =& \bar{x}_n - \bar{x}_{n-1} + \int_0^t \left(v_{\max} - v\left(\frac{\alpha_n^N L}{N(x_n(s) - x_{n-1}(s))} \right) \right) ds \\ \geq& \bar{x}_n - \bar{x}_{n-1} \geq \frac{\alpha_{n-1}^N L}{NM}. \end{aligned}$$

- Assume property is verified for $j+1$ and prove it is still satisfied for j

$$\inf_{0<t\leq T} [x_{j+2}(t) - x_{j+1}(t)] \geq \frac{\alpha_{j+1}^N L}{NM}. \tag{15}$$

Sketch of proof

- By contradiction, assume that there exists $0 \leq t_1 < t_2$ such that

$$\begin{cases} x_{j+1}(t) - x_j(t) \geq \frac{\alpha_j^N L}{NM}, & t < t_1 \\ x_{j+1}(t) - x_j(t) = \frac{\alpha_j^N L}{NM}, & t = t_1 \\ x_{j+1}(t) - x_j(t) < \frac{\alpha_j^N L}{NM}, & t_1 < t \leq t_2. \end{cases} \tag{16}$$

Sketch of proof

- By contradiction, assume that there exists $0 \leq t_1 < t_2$ such that

$$\begin{cases} x_{j+1}(t) - x_j(t) \geq \frac{\alpha_j^N L}{NM}, & t < t_1 \\ x_{j+1}(t) - x_j(t) = \frac{\alpha_j^N L}{NM}, & t = t_1 \\ x_{j+1}(t) - x_j(t) < \frac{\alpha_j^N L}{NM}, & t_1 < t \leq t_2. \end{cases} \tag{16}$$

- Since v is decreasing

$$\begin{aligned} x_j(t) =& x_j(t_1) + \int_{t_1}^{t} v\left(\frac{\alpha_j^N L}{N(x_{j+1}(s) - x_j(s))}\right) ds \\ \leq& x_j(t_1) + v\left(M\right)\left(t - t_1\right), \end{aligned}$$

- Moreover from (15), for $t_1 < t \leq t_2$,

$$\begin{aligned} x_{j+1}(t) =& x_{j+1}(t_1) + \int_{t_1}^{t} v\left(\frac{\alpha_{j+1}^N L}{N(x_{j+2}(s) - x_{j+1}(s))}\right) ds \\ \geq& x_{j+1}(t_1) + v\left(M\right)\left(t - t_1\right) \end{aligned}$$

$$\Rightarrow x_{j+1}(t) - x_j(t) \geq x_{j+1}(t_1) - x_j(t_1) = \frac{\alpha_j^N L}{NM}$$

which contradicts (16), so that (14) is satisfied.

Sketch of proof

- Show upper bound for $i = 0, \dots, n-1$ and $t \in [0, T]$
- Recalling assumptions on v and applying system's dynamics

$$
\begin{aligned}
x_{i+1}(t) - x_i(t) &= x_{i+1}(0) - x_i(0) + \int_0^t (\dot{x}_{i+1}(s) - \dot{x}_i(s)) \, ds \\
&\leq \bar{x}_{i+1} - \bar{x}_i + \int_0^t \left(v_{\max} - v\left(\frac{\alpha_i^N L}{N(x_{i+1}(s) - x_i(s))} \right) \right) ds \\
&\leq \bar{x}_n - \bar{x}_0 + (v_{\max} - v(M))\, t,
\end{aligned}
$$

- Last equality is obtained from lower bound $\Rightarrow$ proof is complete

- Physical conditions on $\alpha := \alpha^N$ induce feasible set

$$\mathcal{A}_N := \left\{ \alpha \in \mathbb{R}^n : \quad \alpha_i \in \left[1, \bar{z}_i^N\right], \quad i = 0, \dots, n-1, \quad \sum_{i=0}^{n-1} \alpha_i = N \right\} \tag{17}$$

with $\bar{z}_i^N := \min \left\{ \frac{N\left(\bar{x}_{i+1}^N - \bar{x}_i^N\right)}{L}, \frac{N\left(\bar{y}_{i+1}^N - \bar{y}_i^N\right)}{L} \right\}, \quad i = 0, \dots, n-1$

[8] Baloul, Hayat, Liard, and Lissy 2025.

ODE-Contrained Optimization

- Physical conditions on $\alpha := \alpha^N$ induce feasible set

$$\mathcal{A}_N := \left\{ \alpha \in \mathbb{R}^n : \quad \alpha_i \in \left[1, \bar{z}_i^N\right], \quad i = 0, \dots, n-1, \quad \sum_{i=0}^{n-1} \alpha_i = N \right\} \tag{17}$$

with $\bar{z}_i^N := \min \left\{ \frac{N\left(\bar{x}_{i+1}^N - \bar{x}_i^N\right)}{L}, \frac{N\left(\bar{y}_{i+1}^N - \bar{y}_i^N\right)}{L} \right\}, \quad i = 0, \dots, n-1$

- **Approximate density reconstruction**[8] $\Rightarrow$ find optimal interaction parameter α

$$\begin{aligned} & \underset{\alpha}{\text{minimize}} \quad \frac{1}{2} \|x(T) - \bar{y}\|^2 \\ \text{s.t.} \quad & \dot{x}(t) = V\left(W_\alpha x(t) + b_\alpha(t)\right) \\ & x(0) = \bar{x} \\ & \alpha \in \mathcal{A}_N \end{aligned} \tag{18}$$

[8] Baloul, Hayat, Liard, and Lissy 2025.

- Physical conditions on $\alpha := \alpha^N$ induce feasible set

$$\mathcal{A}_N := \left\{ \alpha \in \mathbb{R}^n : \quad \alpha_i \in \left[1, \bar{z}_i^N\right], \quad i = 0, \ldots, n-1, \quad \sum_{i=0}^{n-1} \alpha_i = N \right\} \tag{17}$$

with $\bar{z}_i^N := \min \left\{ \frac{N\left(\bar{x}_{i+1}^N - \bar{x}_i^N\right)}{L}, \frac{N\left(\bar{y}_{i+1}^N - \bar{y}_i^N\right)}{L} \right\}, \quad i = 0, \ldots, n-1$

- **Approximate density reconstruction**[8] $\Rightarrow$ find optimal interaction parameter α

$$\begin{aligned} & \underset{\alpha}{\text{minimize}} \quad \frac{1}{2} \left\| x(T) - \bar{y} \right\|^2 \\ \text{s.t.} \quad & \dot{x}(t) = V\left(W_\alpha x(t) + b_\alpha(t)\right) \\ & x(0) = \bar{x} \\ & \alpha \in \mathcal{A}_N \end{aligned} \tag{18}$$

- Existence of solutions guaranteed by assumptions on $V := v \circ \frac{1}{\cdot}$ (continuity of v) and constraints on α (compactness of $\mathcal{A}_N$)

[8] Baloul, Hayat, Liard, and Lissy 2025.

ODE-Contrained Optimization

- Physical conditions on $\alpha := \alpha^N$ induce feasible set

$$\mathcal{A}_N := \left\{ \alpha \in \mathbb{R}^n : \quad \alpha_i \in \left[1, \bar{z}_i^N\right], \quad i = 0, \dots, n-1, \quad \sum_{i=0}^{n-1} \alpha_i = N \right\} \tag{17}$$

with $\bar{z}_i^N := \min \left\{ \frac{N\left(\bar{x}_{i+1}^N - \bar{x}_i^N\right)}{L}, \frac{N\left(\bar{y}_{i+1}^N - \bar{y}_i^N\right)}{L} \right\}, \quad i = 0, \dots, n-1$

- **Approximate density reconstruction**[8] $\Rightarrow$ find optimal interaction parameter α

$$\begin{aligned} &\underset{\alpha}{\text{minimize}} \quad \frac{1}{2} \left\| x(T) - \bar{y} \right\|^2 \\ \text{s.t.} \quad &\dot{x}(t) = V\left(W_\alpha x(t) + b_\alpha(t)\right) \\ &x(0) = \bar{x} \\ &\alpha \in \mathcal{A}_N \end{aligned} \tag{18}$$

- Existence of solutions guaranteed by assumptions on $V := v \circ \frac{1}{\cdot}$ (continuity of v) and constraints on α (compactness of $\mathcal{A}_N$)
- No uniqueness (a priori) since nonlinear dynamics can lead to multiple minima

[8] Baloul, Hayat, Liard, and Lissy 2025.

Learning Method

- Dataset consists of **artificial data** based on simulated (classical) FtL dynamics (5)
- Sampling of PVs yielding a **balanced representation** of overall traffic

Learning Method

- Dataset consists of **artificial data** based on simulated (classical) FtL dynamics (5)
- Sampling of PVs yielding a **balanced representation** of overall traffic
- Neural network architecture designed to **understand dynamics of traffic**

- Dataset consists of **artificial data** based on simulated (classical) FtL dynamics (5)
- Sampling of PVs yielding a **balanced representation** of overall traffic
- Neural network architecture designed to **understand dynamics of traffic**
- Residual network (ResNet) where each block corresponds to a single time step
- Input $\bar{x}$ and state $x(.)$ is propagated by mirroring Euler discretization

$$x(t+\Delta t) = x(t) + V(Wx(t)+b)\Delta t \tag{19}$$

- Weights and biases W, b are functions of α

$$\begin{cases} W_{i,i} & := -\frac{N}{\alpha_i L}, i = 0, \dots, n-1, \\ W_{i,i+1} & := \frac{N}{\alpha_i L}, i = 1, \dots, n-2, \\ W_{i,j} & := 0, \text{otherwise}, \end{cases} \tag{20}$$

$$b_i(t) =:= \delta_{i,n} \frac{N}{\alpha_{n-1} L} \left(v_{\max} t + \bar{x}_n^N \right), \quad t \in [0, T] \tag{21}$$

- Nonlinear dynamic map V acts as physics grounded activation function
- Backpropagation to minimize predictions errors $\frac{1}{n} \sum_{j=0}^{n} |x_j^{\alpha}(T) - \bar{y}_j^N|^2$

Learning Architecture

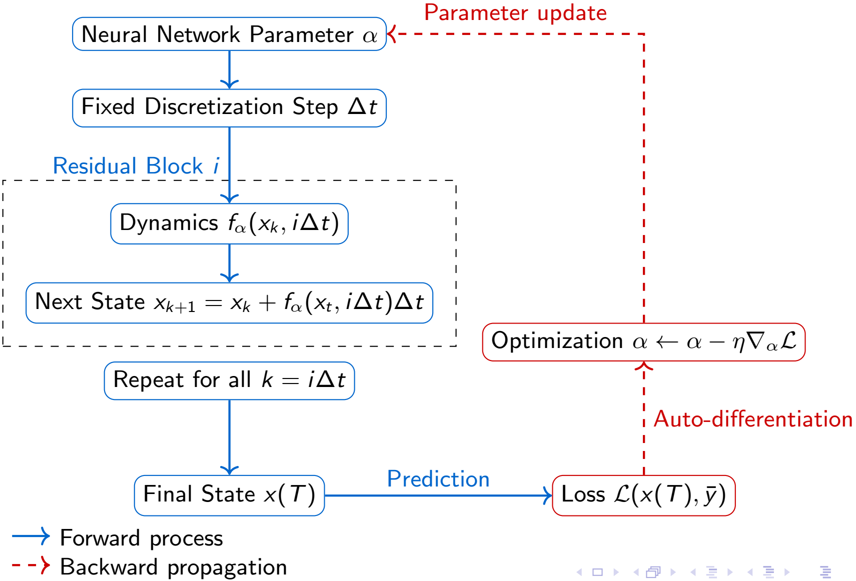

Model validation

- Through predicted parameter $\bar{\alpha}$, training yields piecewise constant discrete density

$$\rho^N(t,x) = \sum_{i=0}^{n-1} \frac{\bar{\alpha}_i L}{N(x_{i+1}^N(t) - x_i^N(t))} \chi_{[x_i^N(t), x_{i+1}^N(t))}(x), \quad x \in \mathbb{R}, \quad t \in [0,T], \tag{22}$$

- Through predicted parameter $\bar{\alpha}$, training yields piecewise constant discrete density

$$\rho^N(t,x) = \sum_{i=0}^{n-1} \frac{\bar{\alpha}_i L}{N(x_{i+1}^N(t) - x_i^N(t))} \chi_{[x_i^N(t), x_{i+1}^N(t))}(x), \quad x \in \mathbb{R}, \quad t \in [0,T], \tag{22}$$

- Simulation on **test data** by solving ODE system

$$\begin{cases} \dot{x}_i^N(t) = v\left(\rho^N(t, x_i(t)^+)\right), & t \in (0,T], \\ x_i^N(0) = \bar{x}_i^N & i = 0, \dots, n_{\text{test}} \end{cases} \tag{23}$$

Model validation

- Through predicted parameter $\bar{\alpha}$, training yields piecewise constant discrete density

$$\rho^N(t,x) = \sum_{i=0}^{n-1} \frac{\bar{\alpha}_i L}{N(x_{i+1}^N(t) - x_i^N(t))} \chi_{[x_i^N(t), x_{i+1}^N(t))}(x), \quad x \in \mathbb{R}, \quad t \in [0,T], \tag{22}$$

- Simulation on **test data** by solving ODE system

$$\begin{cases} \dot{x}_i^N(t) = v\left(\rho^N(t, x_i(t)^+)\right), & t \in (0,T], \\ x_i^N(0) = \bar{x}_i^N & i = 0, \dots, n_{\text{test}} \end{cases} \tag{23}$$

- Assess model's performance by measuring test error $\frac{1}{n_{\text{test}}} \sum_{j=0}^{n_{\text{test}}} |x_j(T) - \bar{y}_i^N|^2$

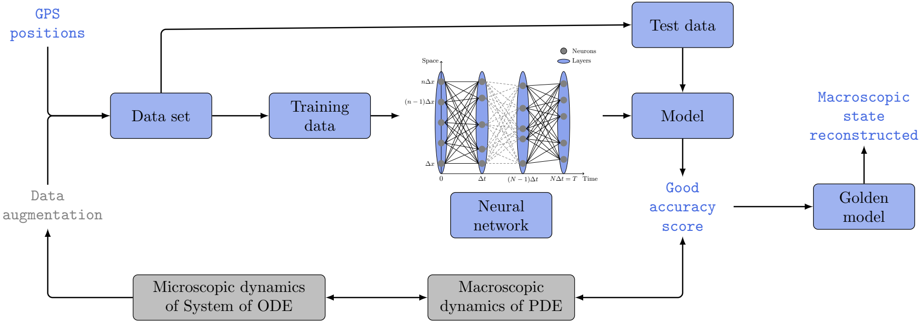

Traffic Flow Reconstruction Pipeline

Table of Contents

Outline of Convergence Analysis

- Prove that, **if only using data from dynamical systems**, approximate density ρ^N predicted by our machine learning model converges to solution of the LWR model (6) when the number of vehicles approaches infinity

Outline of Convergence Analysis

- Prove that, **if only using data from dynamical systems**, approximate density ρ^N predicted by our machine learning model converges to solution of the LWR model (6) when the number of vehicles approaches infinity
- Main challenge lies in imposing a condition on distribution of α which would guarantee convergence

Outline of Convergence Analysis

- Prove that, **if only using data from dynamical systems**, approximate density ρ^N predicted by our machine learning model converges to solution of the LWR model (6) when the number of vehicles approaches infinity
- Main challenge lies in imposing a condition on distribution of α which would guarantee convergence
- Demonstrate that discrete initial density $\rho^N(0, \cdot)$ converges to the initial condition $\bar{\rho}$ in the LWR model (6) under this additional assumption

Outline of Convergence Analysis

- Prove that, **if only using data from dynamical systems**, approximate density ρ^N predicted by our machine learning model converges to solution of the LWR model (6) when the number of vehicles approaches infinity
- Main challenge lies in imposing a condition on distribution of α which would guarantee convergence
- Demonstrate that discrete initial density $\rho^N(0,\cdot)$ converges to the initial condition $\bar{\rho}$ in the LWR model (6) under this additional assumption
- In addition to Euler discrete density (11), consider empirical discrete density

$$\widehat{\rho}^N(t,\cdot) := \frac{L}{N}\sum_{i=0}^{n-1} \alpha_i^N \delta_{x_i(t)}(\cdot), \quad t \in [0,T]. \tag{24}$$

- Prove that, **if only using data from dynamical systems**, approximate density ρ^N predicted by our machine learning model converges to solution of the LWR model (6) when the number of vehicles approaches infinity
- Main challenge lies in imposing a condition on distribution of α which would guarantee convergence
- Demonstrate that discrete initial density $\rho^N(0,\cdot)$ converges to the initial condition $\bar{\rho}$ in the LWR model (6) under this additional assumption
- In addition to Euler discrete density (11), consider empirical discrete density

$$\widehat{\rho}^N(t,\cdot) := \frac{L}{N}\sum_{i=0}^{n-1} \alpha_i^N \delta_{x_i(t)}(\cdot), \quad t \in [0,T]. \tag{24}$$

- **Important observation**: by construction, initial traffic density must satisfy

$$\bar{x}_{i+1} = \sup\left\{x \in \mathbb{R} : \int_{\bar{x}_i}^{x} \bar{\rho}(y)dy \leq \frac{\alpha_i L}{N}\right\}, \quad i = 0,\ldots,n-1 \tag{25}$$

$\Rightarrow$ although no access to ground-truth initial car density $\bar{\rho}$, initial positions $\bar{x}_i$ of probe vehicles verify (25) (i.e. number of unobserved vehicles between $[x_i, x_{i+1})$ is given by α_i)

- Weak solution of (6) is entropy admissible if it satisfies **Kruzhkov entropy condition**

$$\int_0^T \int_{\mathbb{R}} |u-k| \frac{\partial \phi}{\partial t} + \mathrm{sign}(u-k)(f(u)-f(k)) \frac{\partial \phi}{\partial x} dxdt \geq 0, \quad \forall k \in \mathbb{R} \tag{26}$$

Theorem Convergence of approximate density to solution of LWR

Under some assumptions, piecewise-constant density

$$\rho^N(t,x) = \sum_{i=0}^{n-1} \frac{\bar{\alpha}_i^N L}{N(x_{i+1}^N(t) - x_i^N(t))} \chi_{[x_i^N(t), x_{i+1}^N(t))}(x), \quad x \in \mathbb{R}, \quad t \in [0,T], \tag{27}$$

where $\bar{\alpha}_i^N \in \mathcal{A}_N$ is a solution to (18) converges to **unique entropy** solution ρ of

$$\begin{aligned} &\frac{\partial \rho}{\partial t}(t,x) + \frac{\partial f(\rho)}{\partial x}(t,x) = 0, \quad x \in \mathbb{R}, \quad t \in [0,T], \\ &\rho(0,x) = \bar{\rho}(x), \quad x \in \mathbb{R} \end{aligned} \tag{28}$$

- Weak solution of (6) is entropy admissible if it satisfies **Kruzhkov entropy condition**

$$\int_0^T \int_{\mathbb{R}} |u-k|\frac{\partial \phi}{\partial t} + \operatorname{sign}(u-k)(f(u)-f(k))\frac{\partial \phi}{\partial x} dxdt \geq 0, \quad \forall k \in \mathbb{R} \tag{26}$$

Theorem Convergence of approximate density to solution of LWR

Under some assumptions, piecewise-constant density

$$\rho^N(t,x) = \sum_{i=0}^{n-1} \frac{\bar{\alpha}_i^N L}{N(x_{i+1}^N(t) - x_i^N(t))} \chi_{[x_i^N(t), x_{i+1}^N(t))}(x), \quad x \in \mathbb{R}, \quad t \in [0,T], \tag{27}$$

where $\bar{\alpha}_i^N \in \mathcal{A}_N$ is a solution to (18) converges to **unique entropy** solution ρ of

$$\begin{aligned} &\frac{\partial \rho}{\partial t}(t,x) + \frac{\partial f(\rho)}{\partial x}(t,x) = 0, \quad x \in \mathbb{R}, \quad t \in [0,T], \\ &\rho(0,x) = \bar{\rho}(x), \quad x \in \mathbb{R} \end{aligned} \tag{28}$$

- Impose a condition that ensures controlled growth of α_N

Sketch of proof

- Ensures discretization aligns consistently with true initial density when $N \to \infty$
- Notations: for $t \in [0, T]$, $\rho(t) := \rho(t, \cdot)$ and $\widehat{\rho}(t) := \widehat{\rho}(t, \cdot)$.
  In particular, at $t = 0$, $\rho(0) := \rho(0, \cdot)$ and $\widehat{\rho}(0) := \widehat{\rho}(0, \cdot)$

Sketch of proof

- Ensures discretization aligns consistently with true initial density when $N \to \infty$
- Notations: for $t \in [0, T]$, $\rho(t) \coloneqq \rho(t, \cdot)$ and $\widehat{\rho}(t) \coloneqq \widehat{\rho}(t, \cdot)$.
  In particular, at $t = 0$, $\rho(0) \coloneqq \rho(0, \cdot)$ and $\widehat{\rho}(0) \coloneqq \widehat{\rho}(0, \cdot)$
- Use **Wasserstein distance** defined in Di Francesco and Rosini 2015 by

$$\mathrm{W}_{L,1}(f, g) = \|f(]-\infty, \cdot]) - g(]-\infty, \cdot]\|_{L^1(\mathbb{R},\mathbb{R})} \tag{29}$$

Proposition

Let $\bar{\rho}$ satisfy (25) and assume that

$$\max_{i=0,\dots,n-1} \alpha_i^N = o(N) \tag{30}$$

Then, both sequences $(\rho^N(0))_{n\in\mathbb{N}}$ and $(\widehat{\rho}^N(0))_{n\in\mathbb{N}}$ converge to $\bar{\rho}$ in the sense of the $\mathrm{W}_{L,1}$ -Wasserstein distance in (29)

Remark

A particular case of assumption (30) is when $\max_{i=0,\dots,n-1} \alpha_i^N \leq \frac{CN}{\log(N)}$ for some $C > 0$

Sketch of proof

- Using $l_N := L/N$, $\mathrm{W}_{L,1}$- distance and discrete density in (10)

$$\begin{aligned} \mathrm{W}_{L,1}(\rho^N(0), \widehat{\rho}^N(0)) &= \sum_{i=0}^{n-1} \int_{\bar{x}_i}^{\bar{x}_{i+1}^N} \left(\alpha_i^N l_N - \rho_i^N(t)\,(x - \bar{x}_i) \right) dx \\ &= \sum_{i=0}^{n-1} \alpha_i^N l_N \int_{\bar{x}_i}^{\bar{x}_{i+1}} \left(1 - \frac{x - \bar{x}_i}{\bar{x}_{i+1} - \bar{x}_i} \right) dx \\ &\leq \max_{i=0,\ldots,n} \{\alpha_i^N\} l_N \,(\bar{x}_n - \bar{x}_0) \end{aligned} \tag{31}$$

$\Rightarrow$ it suffices to prove that $(\widehat{\rho}^N(0))_{n\in\mathbb{N}}$ converges to $\bar{\rho}$ wrt $\mathrm{W}_{L,1}$- distance

- Using $l_N := L/N$, $\mathrm{W}_{L,1}$- distance and discrete density in (10)

$$\begin{aligned}
\mathrm{W}_{L,1}(\rho^N(0), \widehat{\rho}^N(0)) &= \sum_{i=0}^{n-1} \int_{\bar{x}_i}^{\bar{x}_{i+1}^N} \left(\alpha_i^N l_N - \rho_i^N(t)\,(x-\bar{x}_i)\right) dx \\
&= \sum_{i=0}^{n-1} \alpha_i^N l_N \int_{\bar{x}_i}^{\bar{x}_{i+1}} \left(1 - \frac{x-\bar{x}_i}{\bar{x}_{i+1}-\bar{x}_i}\right) dx \\
&\leq \max_{i=0,\dots,n} \{\alpha_i^N\} l_N\,(\bar{x}_n - \bar{x}_0)
\end{aligned} \tag{31}$$

$\Rightarrow$ it suffices to prove that $(\widehat{\rho}^N(0))_{n\in\mathbb{N}}$ converges to $\bar{\rho}$ wrt $\mathrm{W}_{L,1}$- distance

- Using expressions of both Euler (11) and empirical (24) discrete densities

$$\begin{aligned}
&\mathrm{W}_{L,1}(\widehat{\rho}^N(0), \bar{\rho}) \\
&= \sum_{i=0}^{n-2} \int_{\bar{x}_i}^{\bar{x}_{i+1}} \left(\sum_{j=0}^{i} \alpha_j^N l_N - \int_{-\infty}^{x} \bar{\rho}(y)dy\right) dx + \int_{\bar{x}_{n-1}}^{\bar{x}_n} \left(L - \int_{-\infty}^{x} \bar{\rho}(y)dy\right) dx \\
&= \sum_{i=0}^{n-2} \int_{\bar{x}_i}^{\bar{x}_{i+1}} \left(\left(\sum_{j=0}^{i-1} \alpha_j^N l_N - \int_{\bar{x}_0}^{\bar{x}_i} \bar{\rho}(y)dy\right) + \left(\alpha_i^N l_N - \int_{\bar{x}_i}^{x} \bar{\rho}(y)dy\right)\right) dx \\
&\quad + \int_{\bar{x}_{n-1}}^{\bar{x}_n} \left(\sum_{j=0}^{n-2} \alpha_j^N l_N - \int_{\bar{x}_0}^{\bar{x}_{n-1}} \bar{\rho}(y)dy\right) + \left(\alpha_{n-1}^N l_N - \int_{\bar{x}_{n-1}}^{x} \bar{\rho}(y)dy\right) dx
\end{aligned}$$

- From atomization of initial density (25), deduce

$$
\begin{aligned}
&\mathrm{W}_{L,1}(\widehat{\rho}^N(0), \bar{\rho}) \\
&\leq \sum_{i=0}^{n-2} \int_{\bar{x}_i}^{\bar{x}_{i+1}} \left(\alpha_i^N l_N - \int_{\bar{x}_i}^{x} \bar{\rho}(y)dy \right) dx + \int_{\bar{x}_{n-1}}^{\bar{x}_n} \left(\alpha_{n-1}^N l_N - \int_{\bar{x}_{n-1}}^{x} \bar{\rho}(y)dy \right) dx \\
&= \sum_{i=0}^{n-1} \alpha_i^N l_N \int_{\bar{x}_i}^{\bar{x}_{i+1}} \left(1 - \frac{1}{\alpha_i^N l_N} \int_{\bar{x}_i}^{x} \bar{\rho}(y)dy \right) dx \\
&\leq \max_{i=0,\dots,n} \left\{ \alpha_i^N \right\} l_N (\bar{x}_n - \bar{x}_0)
\end{aligned}
$$

Sketch of proof

- From atomization of initial density (25), deduce

$$
\begin{aligned}
&\mathrm{W}_{L,1}(\widehat{\rho}^N(0), \bar{\rho}) \\
&\leq \sum_{i=0}^{n-2} \int_{\bar{x}_i}^{\bar{x}_{i+1}} \left(\alpha_i^N l_N - \int_{\bar{x}_i}^{x} \bar{\rho}(y) dy \right) dx + \int_{\bar{x}_{n-1}}^{\bar{x}_n} \left(\alpha_{n-1}^N l_N - \int_{\bar{x}_{n-1}}^{x} \bar{\rho}(y) dy \right) dx \\
&= \sum_{i=0}^{n-1} \alpha_i^N l_N \int_{\bar{x}_i}^{\bar{x}_{i+1}} \left(1 - \frac{1}{\alpha_i^N l_N} \int_{\bar{x}_i}^{x} \bar{\rho}(y) dy \right) dx \\
&\leq \max_{i=0,\dots,n} \left\{ \alpha_i^N \right\} l_N (\bar{x}_n - \bar{x}_0)
\end{aligned}
$$

- From assumption (30) and estimate (31), conclude that $(\rho^N(0))_{n\in\mathbb{N}}$ converges to $\bar{\rho}$ in sense of $\mathrm{W}_{L,1}$-Wasserstein distance

- From atomization of initial density (25), deduce

$$
\begin{aligned}
&\mathrm{W}_{L,1}(\widehat{\rho}^N(0), \bar{\rho}) \\
&\leq \sum_{i=0}^{n-2} \int_{\bar{x}_i}^{\bar{x}_{i+1}} \left(\alpha_i^N l_N - \int_{\bar{x}_i}^{x} \bar{\rho}(y)dy \right) dx + \int_{\bar{x}_{n-1}}^{\bar{x}_n} \left(\alpha_{n-1}^N l_N - \int_{\bar{x}_{n-1}}^{x} \bar{\rho}(y)dy \right) dx \\
&= \sum_{i=0}^{n-1} \alpha_i^N l_N \int_{\bar{x}_i}^{\bar{x}_{i+1}} \left(1 - \frac{1}{\alpha_i^N l_N} \int_{\bar{x}_i}^{x} \bar{\rho}(y)dy \right) dx \\
&\leq \max_{i=0,\dots,n} \left\{ \alpha_i^N \right\} l_N(\bar{x}_n - \bar{x}_0)
\end{aligned}
$$

- From assumption (30) and estimate (31), conclude that $(\rho^N(0))_{n\in\mathbb{N}}$ converges to $\bar{\rho}$ in sense of $\mathrm{W}_{L,1}$-Wasserstein distance
- Moreover, by leveraging expression of discrete density (11), generalize convergence to unique entropy solution of conservation law (6), referring to Di Francesco and Rosini 2015, Theorem 3 $\Rightarrow$ require only minor modifications to original arguments

Table of Contents

- Parameters
  - Maximum traffic speed $v_{\text{max}} = 120$ km/h
  - Maximum traffic density $\rho_{\text{max}} = 200$ cars/km
  - Greenshields velocity $v(\rho) = v_{\text{max}} \max\left\{1 - \frac{\rho}{\rho_{max}}, 0\right\}, \quad \rho \in [0, \rho_{max}]$
  - Final time horizon $T = 0.1$ h
- Sampling such 10% **of total fleet serve as PVs for training and** 2.5% **for testing**

Numerical experiments

- Parameters
  - Maximum traffic speed $v_{\max} = 120$ km/h
  - Maximum traffic density $\rho_{\max} = 200$ cars/km
  - Greenshields velocity $v(\rho) = v_{\max} \max\left\{1 - \frac{\rho}{\rho_{max}}, 0\right\}, \quad \rho \in [0, \rho_{max}]$
  - Final time horizon $T = 0.1$ h
- Sampling such 10% **of total fleet serve as PVs for training and** 2.5% **for testing**
- Three traffic scenarii modelled
  1. Shock wave represents an abrupt transition in traffic conditions
  2. Rarefaction wave represents a smooth transition in traffic condition
  3. Stop-and-go wave characterized by alternating regions of congestion and free flow

Shock wave scenario

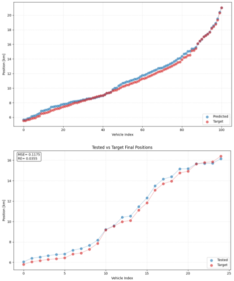

(a) $N = 1000$

Comparison of predicted and target final PV positions
Top Results from **training** procedure
Bottom Results on **test** sounds

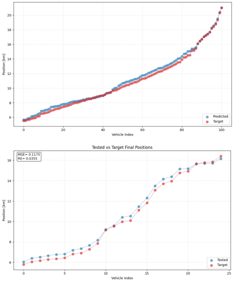

(a) $N = 1000$

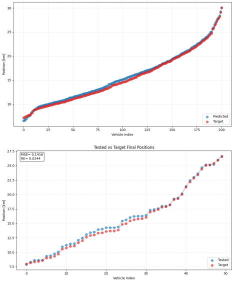

(b) $N = 2000$

Comparison of predicted and target final PV positions
Top Results from **training** procedure
Bottom Results on **test** sounds

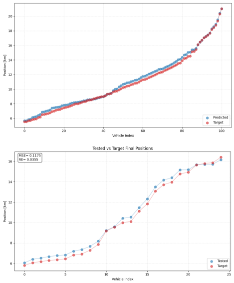

(a) $N = 1000$

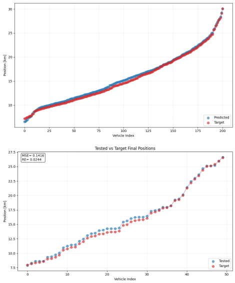

(b) $N = 2000$

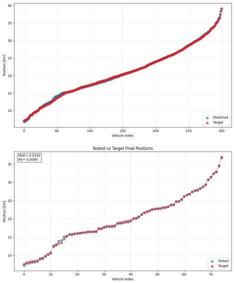

(c) $N = 3000$

Comparison of predicted and target final PV positions
Top Results from **training** procedure
Bottom Results on **test** sounds

Shock wave scenario

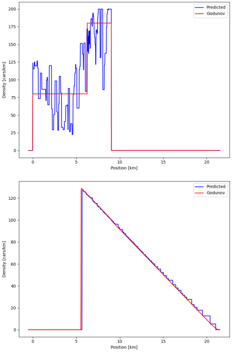

(a) $N = 1000$

Comparison of reconstructed and macroscopic densities
Top Initial densities
Bottom Final densities

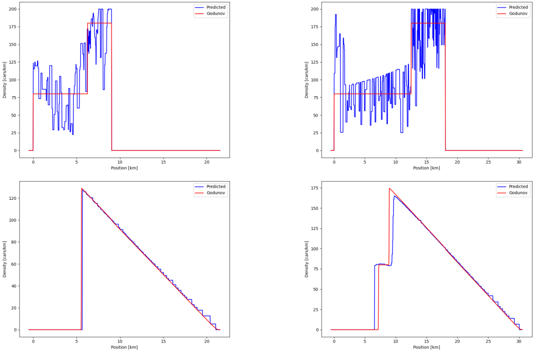

(a) $N = 1000$ (b) $N = 2000$

Comparison of reconstructed and macroscopic densities
Top Initial densities
Bottom Final densities

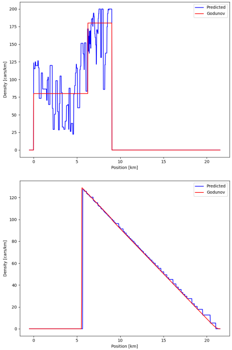

(a) $N = 1000$

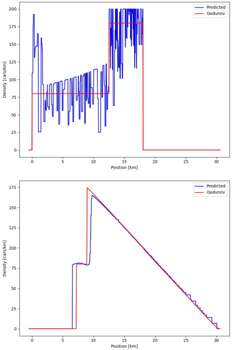

(b) $N = 2000$

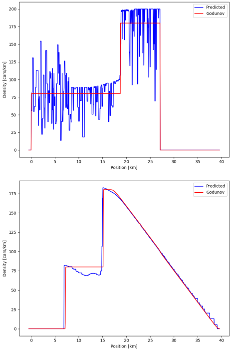

(c) $N = 3000$

Comparison of reconstructed and macroscopic densities
Top Initial densities
Bottom Final densities

Shock wave scenario

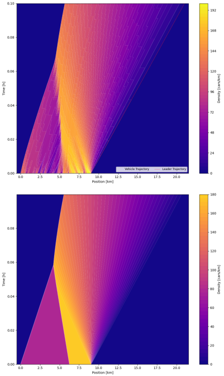

(a) $N = 1000$

Comparison of **reconstructed** and **macroscopic** densities
Top Reconstructed density from learning-based optimization
Bottom Macroscopic density from LWR PDE (Godunov scheme)

Shock wave scenario

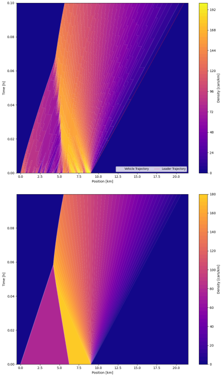

(a) $N = 1000$

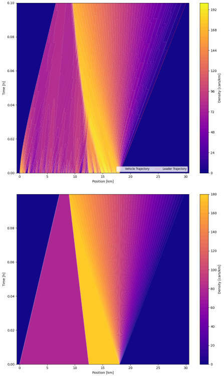

(b) $N = 2000$

Comparison of **reconstructed** and **macroscopic** densities
Top Reconstructed density from learning-based optimization
Bottom Macroscopic density from LWR PDE (Godunov scheme)

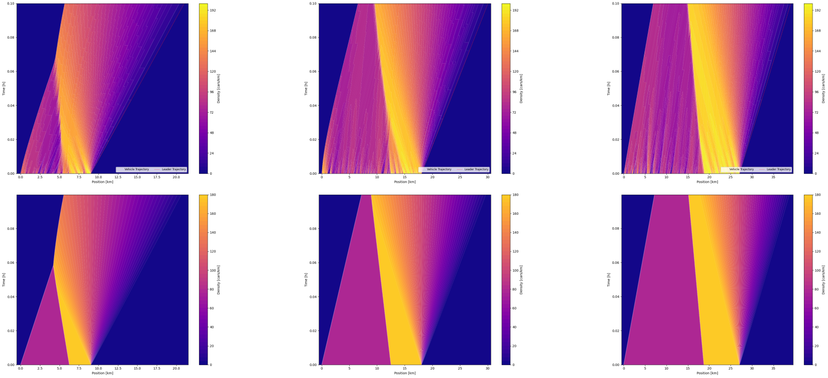

(a) $N = 1000$ (b) $N = 2000$ (c) $N = 3000$

Comparison of **reconstructed** and **macroscopic** densities
Top Reconstructed density from learning-based optimization
Bottom Macroscopic density from LWR PDE (Godunov scheme)

Rarefaction wave scenario

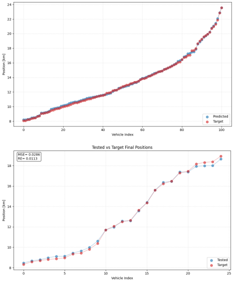

(a) $N = 1000$

Comparison of predicted and target final PV positions
Top Results from **training** procedure
Bottom Results on **test** sounds

Rarefaction wave scenario

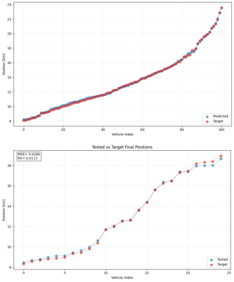

(a) $N = 1000$

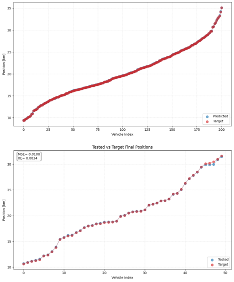

(b) $N = 2000$

Comparison of predicted and target final PV positions
Top Results from **training** procedure
Bottom Results on **test** sounds

Rarefaction wave scenario

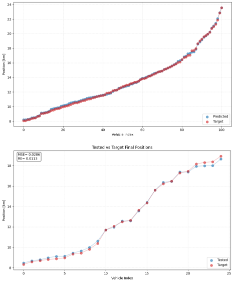

(a) $N = 1000$

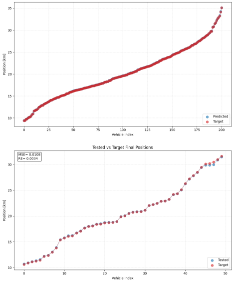

(b) $N = 2000$

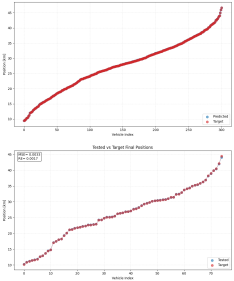

(c) $N = 3000$

Comparison of predicted and target final PV positions
Top Results from **training** procedure
Bottom Results on **test** sounds

Rarefaction wave scenario

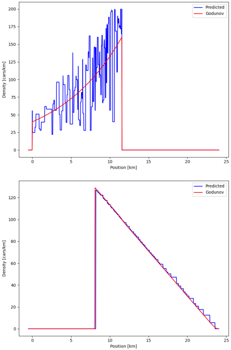

(a) $N = 1000$

Comparison of reconstructed and macroscopic densities
Top Initial densities
Bottom Final densities

Rarefaction wave scenario

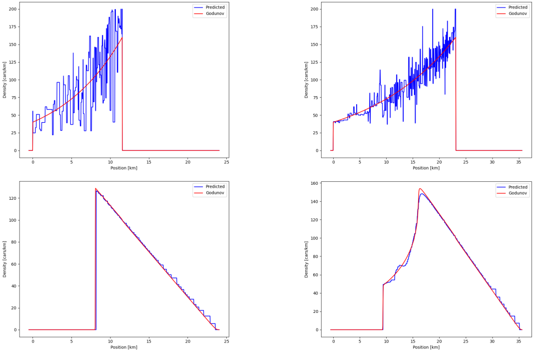

(a) $N = 1000$ (b) $N = 2000$

Comparison of reconstructed and macroscopic densities
Top Initial densities
Bottom Final densities

Rarefaction wave scenario

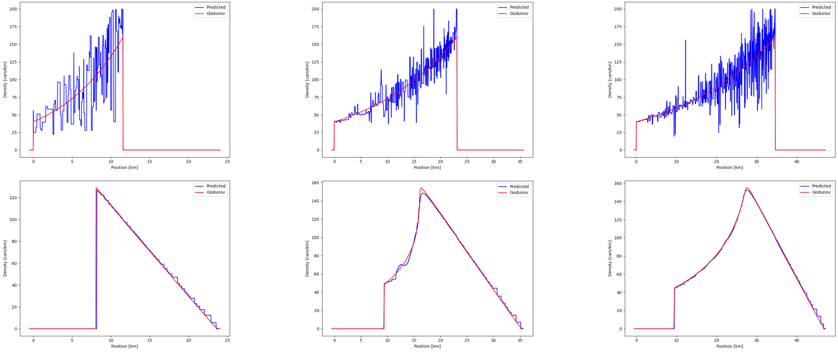

(a) $N = 1000$ (b) $N = 2000$ (c) $N = 3000$

Comparison of reconstructed and macroscopic densities
Top Initial densities
Bottom Final densities

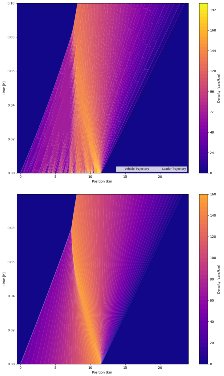

(a) $N = 1000$

Comparison of **reconstructed** and **macroscopic** densities
Top Reconstructed density from learning-based optimization
Bottom Macroscopic density from LWR PDE (Godunov scheme)

Rarefaction wave scenario

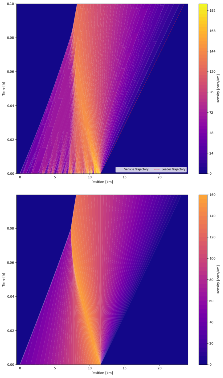

(a) $N = 1000$

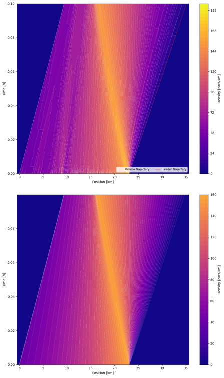

(b) $N = 2000$

Comparison of **reconstructed** and **macroscopic** densities
Top Reconstructed density from learning-based optimization
Bottom Macroscopic density from LWR PDE (Godunov scheme)

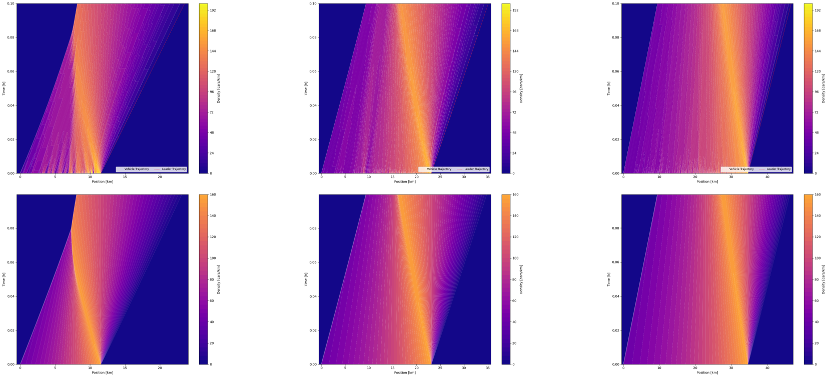

(a) $N = 1000$ (b) $N = 2000$ (c) $N = 3000$

Comparison of **reconstructed** and **macroscopic** densities
Top Reconstructed density from learning-based optimization
Bottom Macroscopic density from LWR PDE (Godunov scheme)

Stop-and-go wave scenario

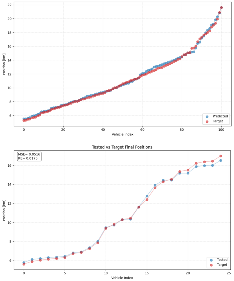

(a) $N = 1000$

Comparison of predicted and target final PV positions
Top Results from **training** procedure
Bottom Results on **test** sounds

Stop-and-go wave scenario

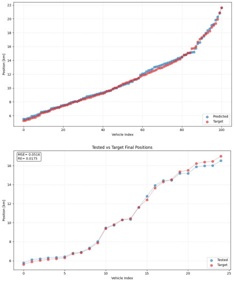

(a) $N = 1000$

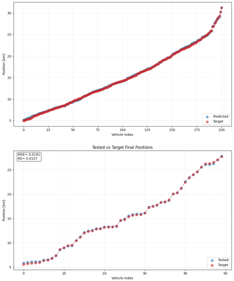

(b) $N = 2000$

Comparison of predicted and target final PV positions
Top Results from **training** procedure
Bottom Results on **test** sounds

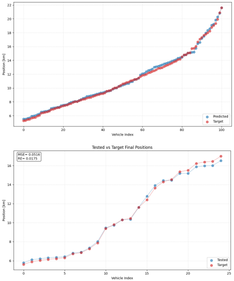

(a) $N = 1000$

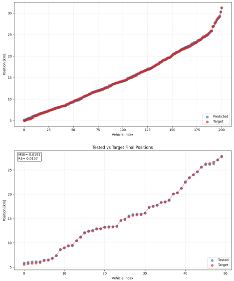

(b) $N = 2000$

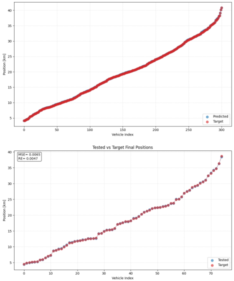

(c) $N = 3000$

Comparison of predicted and target final PV positions
Top Results from **training** procedure
Bottom Results on **test** sounds

Stop-and-go wave scenario

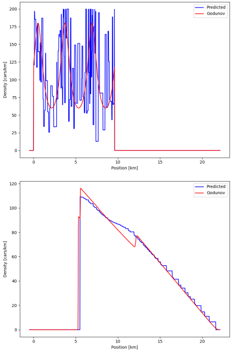

(a) $N = 1000$

Comparison of reconstructed and macroscopic densities
Top Initial densities
Bottom Final densities

Stop-and-go wave scenario

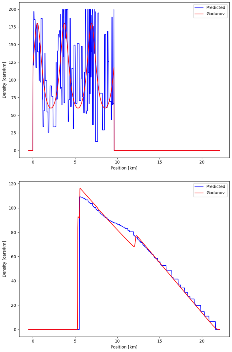

(a) $N = 1000$

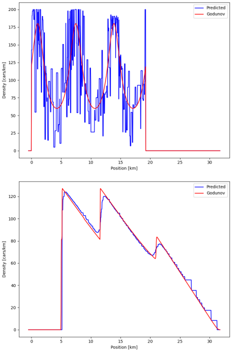

(b) $N = 2000$

Comparison of reconstructed and macroscopic densities
Top Initial densities
Bottom Final densities

Stop-and-go wave scenario

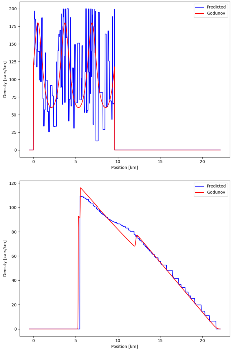

(a) $N = 1000$

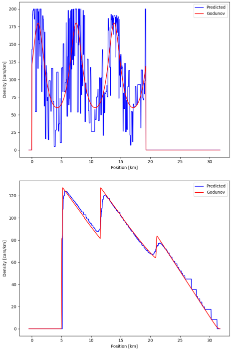

(b) $N = 2000$

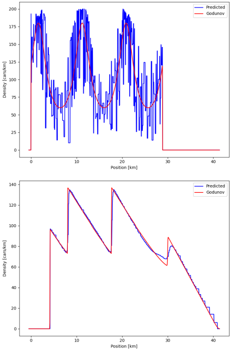

(c) $N = 3000$

Comparison of reconstructed and macroscopic densities
Top Initial densities
Bottom Final densities

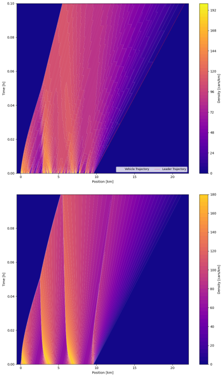

(a) $N = 1000$

Comparison of **reconstructed** and **macroscopic** densities
Top Reconstructed density from learning-based optimization
Bottom Macroscopic density from LWR PDE (Godunov scheme)

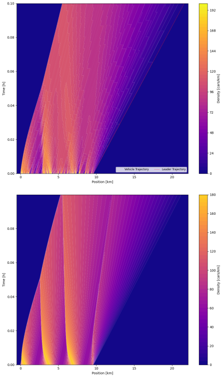

(a) $N = 1000$

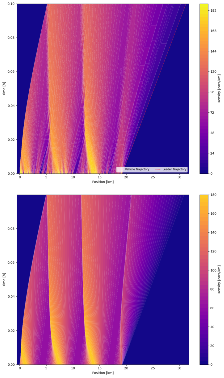

(b) $N = 2000$

Comparison of **reconstructed** and **macroscopic** densities
Top Reconstructed density from learning-based optimization
Bottom Macroscopic density from LWR PDE (Godunov scheme)

Stop-and-go wave scenario

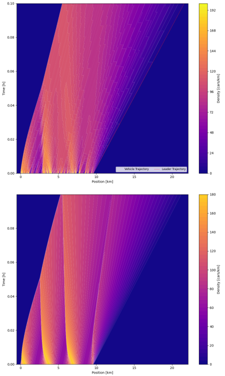

(a) $N = 1000$

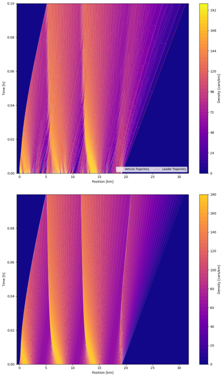

(b) $N = 2000$

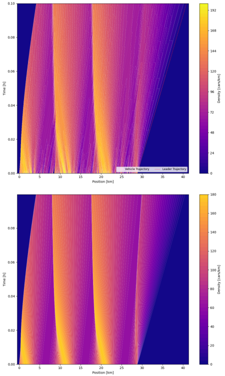

(c) $N = 3000$

Comparison of **reconstructed** and **macroscopic** densities
Top Reconstructed density from learning-based optimization
Bottom Macroscopic density from LWR PDE (Godunov scheme)

Table of Contents

Traffic State Reconstruction Approaches

- Model-Based Method
  - $\Rightarrow$ uses microscopic and macroscopic models
  - $\Rightarrow$ provides theoretical guarantees
  - $\Rightarrow$ struggles to capture real-world complexities
- Data-Driven Method
  - $\Rightarrow$ learns patterns directly from measurement data
  - $\Rightarrow$ derives system properties or predicts near-future states
  - $\Rightarrow$ requires extensive data for effectiveness
- Our Approach
  - $\Rightarrow$ combines models and data to address sparsity and improve realism
  - $\Rightarrow$ **Integrates physical priors with data observations**
  - $\Rightarrow$ achieves reliable traffic reconstruction with limited observations

Perspectives

- Conservation law with unilateral constraint[9] (toll gate)

$$\begin{cases} \text{LWR PDE (6) with} \\ f(\rho(t,0)) \le q(t), & t > 0. \end{cases} \tag{32}$$

- Conservation law with moving bottleneck[10] (slow vehicle)

$$\begin{cases} \text{LWR PDE (6) with} \\ f\left(\rho(t,y(t))\right) - \dot{y}(t)\rho(t,y(t)) \le \frac{\alpha \rho_{\max}}{4 v_{\max}} \left(v_{\max} - \dot{y}(t)\right)^2, & t > 0, \\ \dot{y}(t) = \omega\left(\rho(t, y(t)_+)\right), & t > 0, \\ y(0) = y_0 \end{cases} \tag{33}$$

- Network[11] with a junction[12] J and N incoming roads and M outgoing ones

$$\begin{cases} \partial_t \rho_l(t,x) + \partial_x\left(f(\rho_l(t,x))\right) = 0, & t > 0, \quad x \in I_l, \quad l = 1, \dots, N+M \\ \rho_l(0,x) = \rho_{0,l}(x), & x \in I_l = [a_l, b_l], \quad l = 1, \dots, N+M \end{cases} \tag{34}$$

$\Rightarrow \sum_{i=1}^{N} f\left(\rho_i(t,(b_i)_-)\right) = \sum_{j=N+1}^{N+M} f\left(\rho_j(t,(a_j)_+)\right)$ (Rankine Hugoniot)

$\Rightarrow \sum_{i=1}^{N} f\left(\rho_i(t,(b_i)_-)\right)$ is maximized[13] s.t. $f\left(\rho_j(\cdot,(a_j)_+)\right) = \sum_{i=1}^{N} a_{j,i} f\left(\rho_i(\cdot,(b_i)_-)\right)$

[9] Colombo and Goatin 2007.

[10] Liard and Piccoli 2021.

[11] Monneau 2024.

[12] Coclite, Piccoli, and Garavello 2005.

[13] Garavello and Piccoli 2006.

References I

Baloul, N., A. Hayat, T. Liard, and P. Lissy (2025). "Traffic Flow Reconstruction from Limited Collected Data". In: *hal preprint hal-05042012v1*.

Barreau, M., M. Aguiar, J. Liu, and K. H. Johansson (2021). "Physics-Informed Learning for Identification and State Reconstruction of Traffic Density". In: *arXiv preprint arXiv:2103.13852*.

Coclite, G. M., B. Piccoli, and M. Garavello (2005). "Traffic Flow on a Road Network". In: *SIAM Journal on Mathematical Analysis* 36.6, pp. 1862–1886.

Colombo, R. M. and P. Goatin (2007). "A Well-Posed Conservation Law with a Variable Unilateral Constraint". In: *Journal of Differential Equations* 234.2, pp. 654–675.

Di Francesco, M., S. Fagioli, M. D. Rosini, and G. Russo (2016). "Follow-the-Leader Approximations of Macroscopic Models for Vehicular and Pedestrian Flows". In: *arXiv preprint arXiv:1610.06743*.

Di Francesco, M. and M. D. Rosini (2015). "Rigorous Derivation of Nonlinear Scalar Conservation Laws from Follow-the-Leader Type Models via Many Particle Limit". In: *arXiv preprint arXiv:1404.7062*.

Garavello, M. and B. Piccoli (2006). *Traffic Flow on Networks*. Vol. 1. Applied Mathematics. American Institute of Mathematical Sciences.

References II

Holden, H. and N. H. Risebro (2017). "The Continuum Limit of Follow-the-Leader Models: A Short Proof". In: *arXiv preprint arXiv:1709.07661*.

Liard, T. and B. Piccoli (2021). "On entropic solutions to conservation laws coupled with moving bottlenecks". In: *Communications in Mathematical Sciences* 19.4, pp. 1041–1068.

Liu, J., M. Barreau, M. Cicic, and K. H. Johansson (2020). "Learning-Based Traffic State Reconstruction Using Probe Vehicles". In: *arXiv preprint arXiv:2011.05031*.

Monneau, R (2024). "Structure of Riemann solvers on networks (preliminary version)". In: *hal preprint hal-04764513v1*.